Original Paper

Surface treatment of glass and ceramics using XeCl excimer laser radiation[1])

Claudia Buerhop

Institut für Werkstoffwissenschaften III (Glas und Keramik), Universität Erlangen-Nürnberg, Erlangen (Germany)

Norbert Lutz

Forschungsverbund Lasertechnologie Erlangen, Lehrstuhl für Fertigungstechnologie, Universität Erlangen-Nürnberg, Erlangen (Germany)

Rudolf Weißmann and Gerhard Tomandl

Institut für Werkstoffwissenschaften III (Glas und Keramik), Universität Erlangen-Nürnberg, Erlangen (Germany)

Dedicated to Prof. Dr.-Ing. Rolf Brückner on the occasion of his 65th birthday

A XeCl excimer laser with uniform beam profile and 308 nm wavelength was used for ablation and surface modification of technical glasses and ceramics. The ablation behaviour and the resulting surface morphology of the different materials were measured in dependence upon the energy density and the number of pulses. In contradiction to ceramics, glasses show a higher ablation threshold and considerable higher ablation rates. Due to the short wavelength of the excimer laser, microstructuring of glass and ceramic surfaces is possible. Examples are presented, like marking of glasses, microline structuring of float glass, as well as positive and negative microstructuring of ceramics.

Oberflächenbearbeitung von Glas und Keramik mittels XeCl-Excimer-Laserstrahlung

Ein XeCl-Excimer-Laser mit homogenem Strahlprofil und einer Wellenlänge von 308 nm wurde für den Materialabtrag und zur Oberflächenbearbeitung technischer Gläser und Keramiken eingesetzt. Das Abtragsverhalten und die sich daraus ergebende Oberflächenmorphologie der verschiedenen Materialien wurde in Abhängigkeit von der Energiedichte und der Pulszahl untersucht. Im Gegensatz zu Keramiken zeigen Gläser eine höhere Abtragsschwelle und wesentlich höhere Abtragsraten. Auf Grund der kurzen Wellenlänge des Excimer-Lasers ist eine Mikrostrukturierung von Glas- und Keramikoberflächen möglich. Es werden Beispiele gezeigt, wie Markieren von Gläsern, Erzeugung von Linienstrukturen im Mikrometerbereich auf Floatglas sowie positive und negative Mikrostrukturierungen von Keramiken.

1. Introduction

Excimer lasers are high-power lasers with short pulses (10 to 50 ns), low repetition rates (20 to 1000 Hz), and the pulse energies ranging from 0.1 to 2 J. The laser active medium is composed of an inert gas and a halogenide [1]. By changing the gas composition, the emitted ultraviolet radiation ranges from 193 (ArF laser) to 351 nm (XeF laser). The interaction of the excimer laser beam with materials is completely different compared with already industrially used infrared lasers. Using CO_2- and Nd:YAG lasers the applied energy is converted to thermal energy in the material. This induces a strong temperature rise. Thermally activated processes, melting and evaporation of the material occur. The induced thermal stresses are disadvantageous for treating glass and ceramics; fracture of the workpiece might be caused.

On the other hand, excimer lasers might induce photochemical reactions at the surface due to their short wavelengths (high photon energies). Without the detour of thermal decomposition, chemical bonds are cracked by ionization and dissociation. Due to the uniform beam profile excimer lasers are suited for large-area material treatment without focussing the laser beam [2].

The pulse duration of the excimer lasers is in a nanosecond range. This is advantageous, because the energy, applied within a locally well-defined region, is almost completely used for material removal. Only a negligible part flows as heat into the surrounding material. The consequences are rather low temperature gradients and uncritical stresses. Using focussed beams, very high energy densities can be reached so that nonlinear effects result. Focussing down to submicrometer features is possible.

Due to these reasons, excimer lasers are predominantly used for surface modifications and fast contactless marking. The short wavelength offers the possibility of applications in the area of microstructuring of surfaces in the micrometer range [3 and 4].

The photochemical interaction of intense UV radiation with glasses and ceramics is up to now not understood in detail. Basic phenomena will be presented and briefly discussed. Exemplary applica-

Received January 29, 1993.

[1]) Presented in German at the session of the Technical Committee I of DGG on November 26, 1992, in Freiburg (Germany).

Table 1. Technical data of the XeCl excimer laser

wavelength:	308 nm
pulse duration:	50 ns
pulse energy:	2 J
maximum repetition rate:	20 Hz
beam cross section:	(45 × 55) mm^2
maximum average power:	40 W

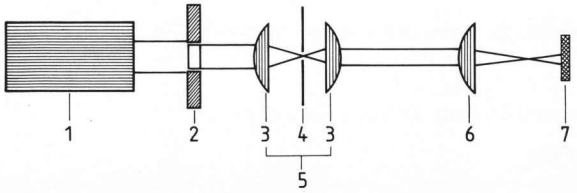

Figure 1. Schematic of mask projection. 1: excimer laser, 2: mask, 3: lens, 4: aperture, 5: telescope, 6: imaging lens, 7: workpiece.

tions on glass and ceramics will be presented in the following sections. More detailed results of the investigations and their discussion will be published shortly.

2. Experimental procedure

For the experiments a XeCl excimer laser (XP2020, Siemens AG, Hamburg (Germany)) was used. Technical data of the laser are shown in table 1. Characteristic for this laser are a large rectangular beam cross section, a homogeneous intensity distribution and a short pulse length in the nanosecond region. The UV exposure of glass and ceramics was carried out using a mask projection scheme, shown in figure 1. Plano-convex fused silica lenses (Suprasil II, L.O.T., Darmstadt (Germany)) were used. The variation of the beam intensity was achieved by a beam splitter of coated fused silica. The resulting energy density on the target was determined with a calorimeter. Using an object imaging ratio of 1:35 of the mask projection energy densities up to 50 J/cm^2 were obtained at the workpiece. This value is equivalent to an irradiance of $4 \cdot 10^7$ W/cm^2.

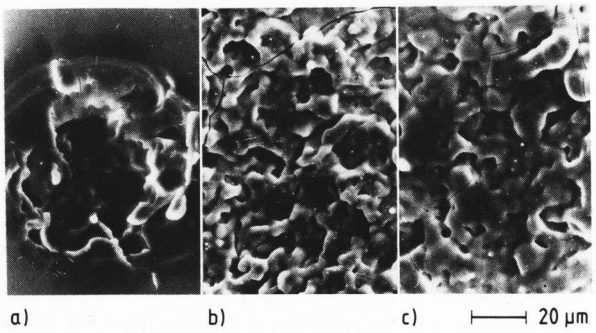

Figures 2a to c. Influence of energy density on float glass surface, treated with 10 pulses, a) $H_E = 10$ J/cm^2, b) $H_E = 20$ J/cm^2, c) $H_E = 50$ J/cm^2,

For the experiments typical commercial glasses and ceramics have been used. Table 2 lists optical and thermal data of these materials. Athermal glass is a normal glass with high iron content (5 wt% Fe_2O_3).

3. Results

3.1. Excimer laser radiation on glass

The modification of the surface morphology using different energy densities is shown in figures 2a to c for float glass as an example. At energy densities close to the ablation threshold, $H_{thr} \approx 10$ J/cm^2, absorption takes place at inhomogeneities and defects. This results in local material removal. Using higher energy densities, material removal occurs homogeneously across the entire irradiated area. The uneven solidified melted phase, which becomes smoother at higher energy densities, is characteristic for float glass.

Table 2. Material properties of different glasses and ceramics

material	refractive index n_d	absorption depth β in µm (at λ = 308 nm)	transformation temperature T_g in °C	linear thermal expansion coefficient α in 10^{-6}/K	melting temperature ϑ_m in °C	sublimation temperature ϑ_{subl} in °C
glass						
fused silica	1.4589	37 000	1 100	0.5		
borosilicate glass	1.473	4 400	568	3.2		
soda–lime–silica glass	1.52	470	530	9.35		
athermal glass	1.54	96	503	8.7		
lead glass	1.55	1 700	465	9.8		
ceramics						
Al_2O_3	1.76			8	2 050	
ZrO_2	2.15			11	≈ 2 700	
Si_3N_4				4		1 900
SiC	2.68			3		≈ 2 700

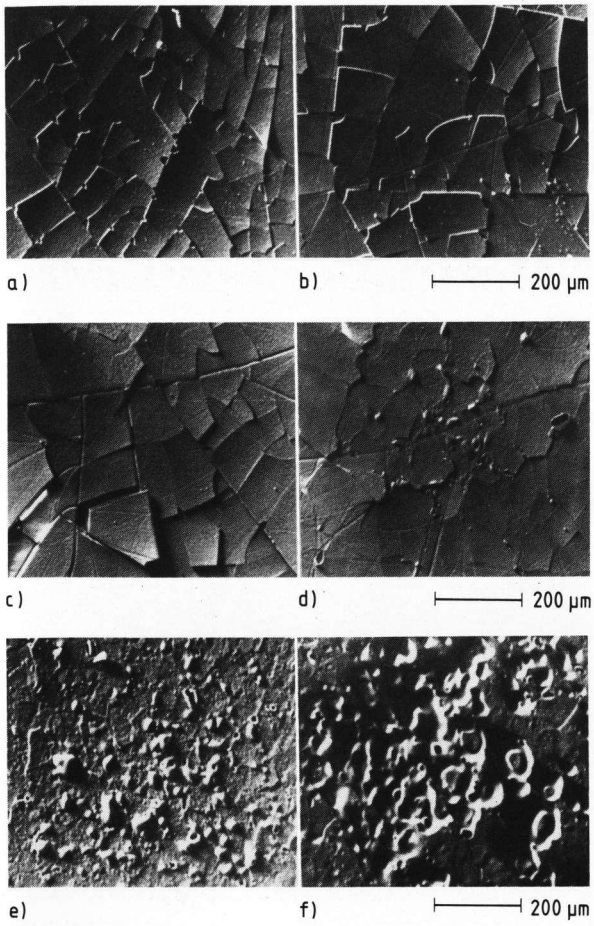

Figures 3a to f. Influence of the number of applied pulses on athermal glass surfaces with an energy density of 9 J/cm^2; a) 2 pulses, b) 10 pulses, c) 20 pulses, d) 30 pulses, e) 50 pulses, f) 100 pulses.

The change of a thermally influenced surface with increasing number of pulses is well-known for athermal glass [5] (figures 3a to f). Due to the induced stress within the thin heated layer, the surface cracks into clods. These segments are shaped according to the induced stress, which depends strongly on the shape of the used mask (square, circle, etc.). Here a circular mask was used. By increasing the number of pulses, the edges of the segments heat up stronger than the inner material because the heat transfer is only possible in one direction. Thus, the edges melt and cracked pieces stick together. As a result cracks are healed superficially. Finally droplets of melt appear on the surface.

The first pictures (figures 2a to c and 3a to f) already indicated that the glass composition plays an important role for the formation of the morphology of the irradiated surface. In figures 4a to d the surfaces of equally treated different glasses are compared. Fused silica is characterized by a rough, sharp-edged surface, which is also typical for borosilicate glass. Soda–lime–silica glass (float glass, athermal glass) and lead glass show different features of thermal effects. The softened volume of float glass

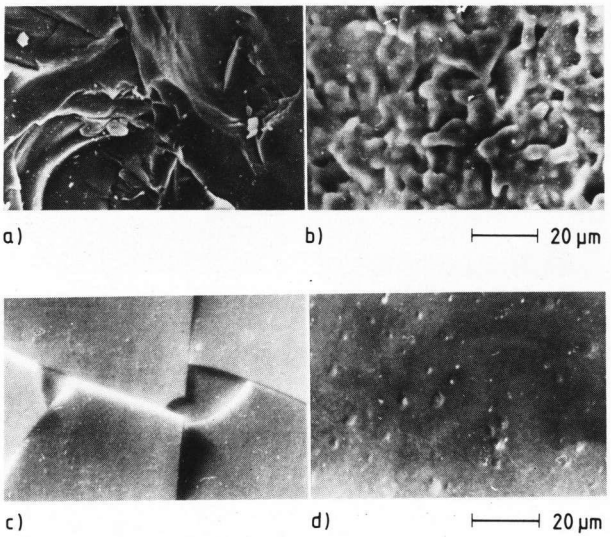

Figures 4a to d. Surfaces of different glasses, H_E = 20 J/cm^2, 10 pulses; a) fused silica, b) float glass, c) athermal glass, d) lead glass.

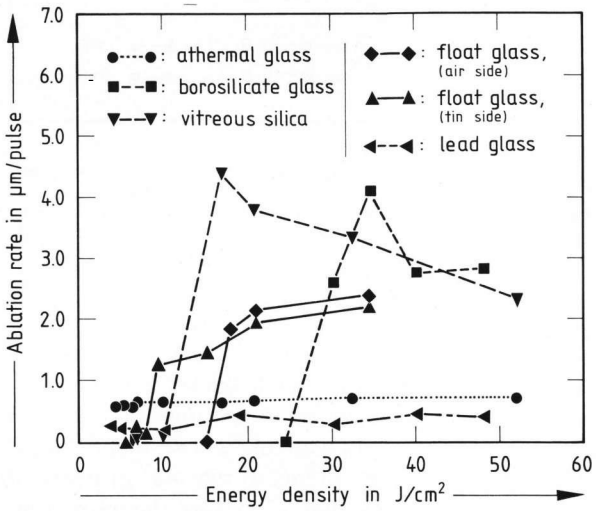

Figure 5. Ablation rate as a function of the energy density of different glasses.

solidifies as an uneven, but smooth surface. A thin surface layer of athermal glass is heated up resulting in a cracked surface. If the transformation temperature is rather low, like for lead glass, a smooth surface results.

Corresponding to the differences in the morphology of the surface, the ablation rate depends also strongly on the properties of the investigated glass. The ablation rate is defined as the derivative of the ablation depth and the number of applied pulses. Figure 5 shows the ablation rates of the investigated glasses. Typical for all glasses is a specific energy density threshold, H_{thr}, above which material removal takes place. Ablation is accompanied by plasma formation. Vitreous silica exhibits a high ablation threshold and a very high ablation rate using energy densities near threshold [6]. Increasing the energy density reduces the ablation rate. A similar behaviour

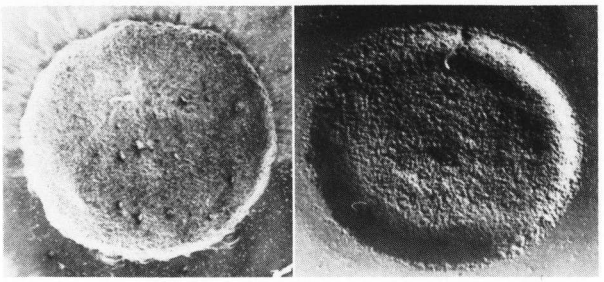

Figures 6a and b. Material removal from float glass surfaces, a) atmosphere side, b) bath side.

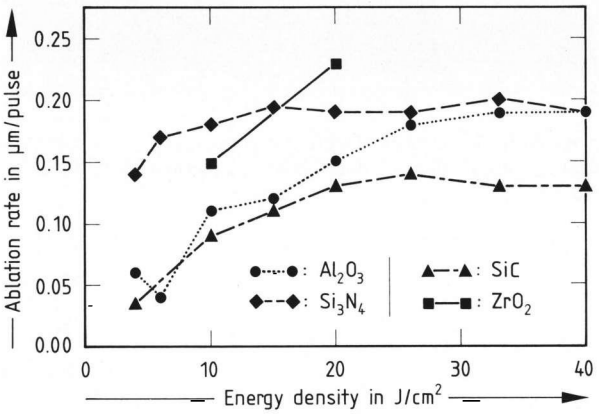

Figure 7. Ablation rate as a function of the energy density of various ceramics.

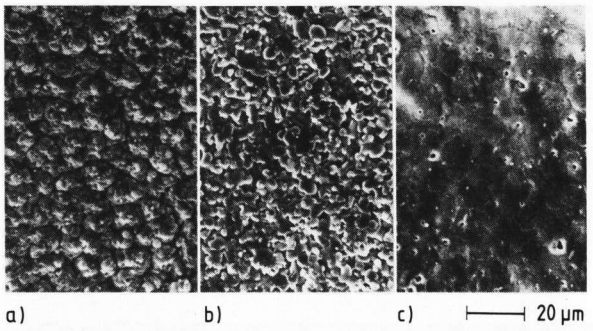

Figures 8a to c. Influence of energy density on the Al_2O_3 surface with 1000 pulses; a) $H_E = 2$ J/cm^2, b) untreated, c) $H_E = 10$ J/cm^2.

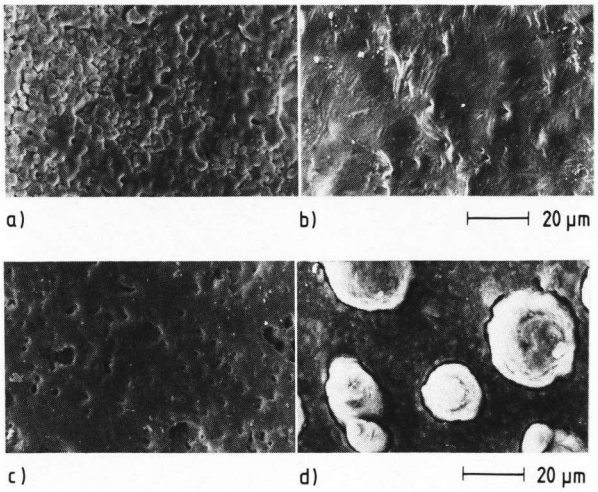

Figures 9a to d. Micrographs of the surfaces of various ceramics with $H_E = 5.2$ J/cm^2; a) Al_2O_3, b) SiC, c) ZrO_2, d) Si_3N_4.

was observed for borosilicate glass. The enormous ablation rate in this energy range might be due to an electrical breakthrough in the glass. Increasing the energy density the induced plasma protects the surface, that means that a part of the radiation is absorbed by the plasma and not in the surface. This results in less material removal. The other glasses with non-bridging oxygen, high alkaline content, and therefore low absorption depth and low transformation temperature have rather low thresholds and low ablation rates. The influence of the absorption of the laser radiation by the induced plasma is less pronounced for these glasses.

Another interesting point is the macroscopic appearance of the irradiated area on float glass. Figures 6a and b show the differing reaction on atmosphere side and bath side. On the atmosphere side the material is removed evenly across the entire irradiated spot, whereas on the bath side the process starts always at the edges and continues towards the centre. This results in a ring-shape pattern on the bath side, which remains visible even for higher pulse numbers. A possible explanation may be that non-linear effects in the high-refractive tin-containing surface lead to self-focussing of the laser beam [5].

3.2. Excimer laser radiation on ceramics

The radiation is absorbed completely in the surface of ceramics, due to surface defects, like grain boundaries, pores, etc., which distinguish crystalline materials from glass. Ablation rates of common oxide and non-oxide ceramics are shown in figure 7. The values are much smaller than those of glasses and the differences are rather minute. The ablation rates of oxides increase with increasing energy density, whereas those of SiC and Si_3N_4 reach a saturation value and become independent of energy density.

Depending strongly on the energy density and the number of applied pulses the surface becomes rougher or smoother than the original untreated surface [7]. Figures 8a to c show the surface of Al_2O_3 treated at two energy densities. At the low energy density (2 J/cm^2), near the ablation threshold, the roughness increases compared to the original surface. Here, ablation takes place, predominantly at grain boundaries, pores, and cracks. Working at the high energy density (10 J/cm^2), the surface becomes smoother. Due to the melted top layer, pores and flaws arise consequently.

Figures 9a to d show different morphologies of oxide and non-oxide ceramics after exposure. Al_2O_3 and ZrO_2 exhibit superficial melting, existence of pores and cracks, although these materials have very high melting temperatures. SiC and Si_3N_4 decompose incongruently, without melting. At high energy densities a wavy surface was observed on Si_3N_4. SiC shows a smooth and sectionally folded surface, which looks like the surface of metallic silicon [8]. This metallic silicon is covered with a high-melting SiO_2 layer, under which the silicon melts. At very high energy densities the surfaces of all the investigated ceramic materials appear even and smooth.

Cross sections of microstructured athermal glass and SiC are presented in figures 10a and b. The steep walls of the holes show the high quality of excimer laser microstructuring. The large depth is important for many applications. Realizing large depths, one has to take into account that the top edges of the walls might be rounded, as observed for athermal glass.

3.3. Discussion

By exceeding a material-specific energy density threshold, material removal starts. This ablation process is accompanied by the formation of a plasma, whose intensity, size, shape, and spectral composition depends on the working parameters and the material. Ablation threshold, ablation rate, and surface morphology are determined by the physical properties of the material and the laser parameters, like energy density, number of applied pulses, pulse repetition rate, and size of the irradiated area.

Table 3 points out clearly that fairly transparent glasses have higher ablation rates than absorbing crystalline ceramic materials. Surface defects, like grain boundaries, pores, etc., support the absorption of laser radiation in ceramics, so that the material removal always starts with the first pulse. In glasses, the ablation process needs several starting pulses, depending on the energy density [9]. During these first pulses the absorption increases due to the creation of internal absorption centres, e.g. colour

Table 3. Maximal ablation rates of different glasses and ceramics

material		ablation rates in µm/pulse
glass	fused silica	3
	borosilicate glass	3
	float glass	2.5
	athermal glass	0.8
	lead glass	0.4
ceramics	Al_2O_3	0.2
	ZrO_2	0.23
	SiC	0.28
	Si_3N_4	0.19

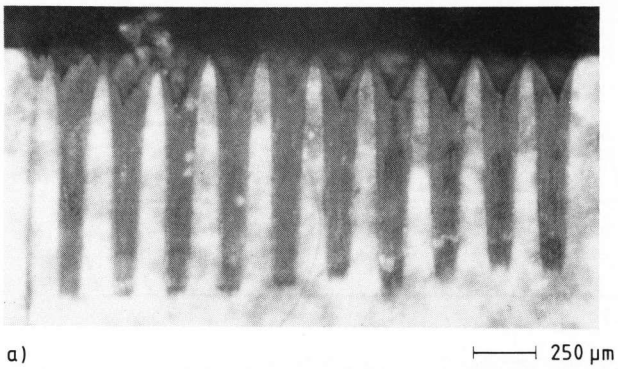

Figures 10a and b. Micrographs of cross sections of a) athermal glass (top), $H_E = 20$ J/cm^2, 1000 pulses, depth = 250 µm, b) SiC (bottom), $H_E = 20$ J/cm^2, 250 pulses, depth = 110 µm.

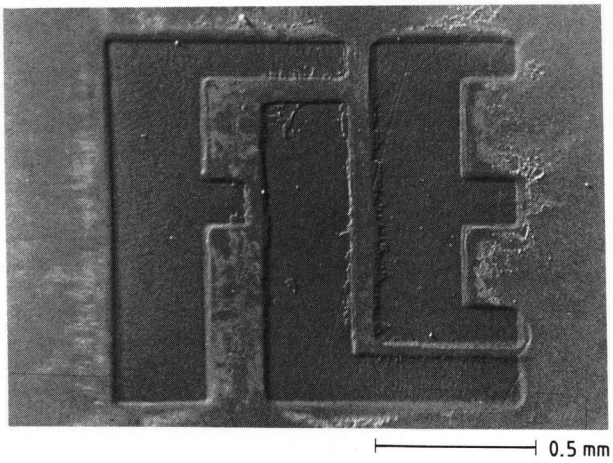

Figure 11. Micrograph of the marking of float glass.

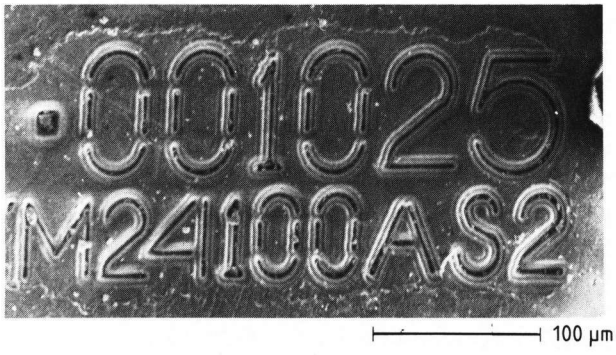

Figure 12. Micrograph of the marking of lead glass.

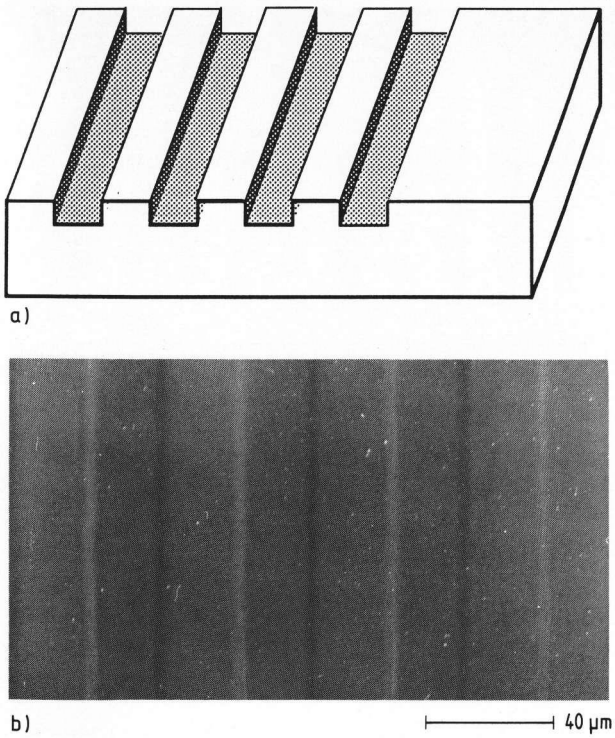

Figures 13a and b. Structure of float glass, a) schematic, b) micrograph.

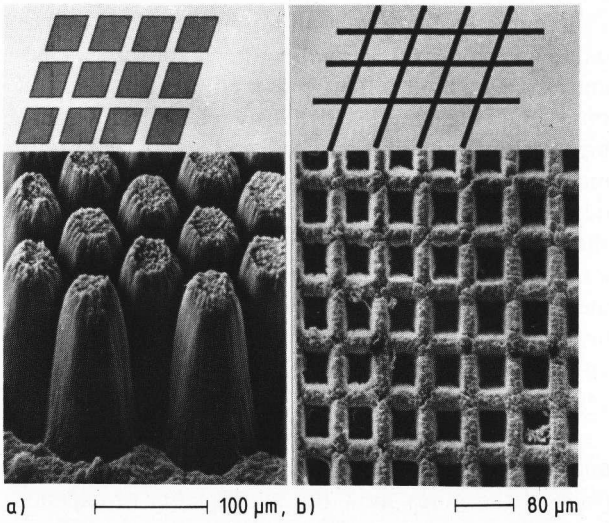

Figures 14a and b. Schematically presented masks and corresponding micrographs showing the microstructuring of ceramics; a) positive structuring of Si_3N_4, 8 J/cm^2, 500 pulses, b) negative structuring of Al_2O_3, 17.5 J/cm^2, 1000 pulses.

centres. Concerning the ablation rates of glasses two groups can be distinguished. The transmitting glasses, fused silica and borosilicate glass, exhibit high ablation thresholds and ablation rates decreasing with increasing energy density. The morphology of the structures is rough, break-outs destroy the edges. Most other glasses have ablation rates which increase rather strongly at the threshold and increase more slightly at higher energy densities. The morphology shows thermal effects.

Because precise microstructuring of most glasses is difficult, if the ablation rate is large, it seems better to use excimer lasers with a shorter wavelength. The radiation of these lasers will be absorbed stronger [10].

4. Applications

Examples for contactless marking of glass surfaces with a few pulses and with a single mask are shown in figures 11 and 12. The letters "F,L,E" (Forschungsverbund Lasertechnologie Erlangen) on float glass are rather large and well-separated by straight edges and clearly defined corners. The other letters on lead glass are much smaller, but still easily to distinguish and readable so that code numbers can be printed easily in the glass without disturbing the macroscopic appearance.

Another application may be the microstructuring of optical layers on the base of SiO_2. Figures 13a and b give a principal idea of the production of plane waveguides, which require dimensions of a few micrometers. Line structures, which satisfy these demands, have been obtained successfully in float glass. The width of the lines presented is about 20 µm, and structures down to 5 µm have recently been realized.

Furthermore, ceramic materials can be structured for special applications. A high resolution of 20 lines per mm and a hole depth of 300 µm were required. Principally two techniques are possible to realize these requirements [11]. The negative technique is to drill holes. The positive technique is to cut grooves in the surface. Figures 14a and b show examples of each technique. In the upper part the necessary masks are presented schematically and below the obtained structure. A part of the material removed from the holes is deposited on top of the side walls, resulting in a rough appearance. The conical shape and the rough top of the Si_3N_4 cylinders are due to erosion as an influence of the plasma.

5. References

[1] Sowada, U.; Lokai, P.; Kahlert, H.-J. et al.: Excimer-laser-Bearbeitung keramischer Werkstoffe. Ergebnisse und physikalische Vorgänge. Laser Optoelektron. **21** (1989) no. 3, p. 107–115.

[2] Sowada, U.; Kahlert, H.-J.; Basting, D.: Excimer-laser material processing – Methods and results. Laser Optoelektron. **20** (1988) no. 2, p. 96–101.

[3] Tönshoff, H. K.; Gedrat, O.: Removal process of ceramic materials with excimer laser radiation. SPIE **1132** (1989) p. 104–110.

[4] Tönshoff, H. K.; Gedrat, O.: Absorption behaviour of ceramic materials irradiated with excimer-lasers. SPIE **1377** (1991) p. 38–44.

[5] Buerhop, C.; Weissmann, R.: Precise marking of silicate glass

by excimer-laser and TEA-CO_2-laser irradiation. In: XVI International Congress on Glass, Madrid (Spain) 1992. Vol. 4. p. 211–218.

[6] Ihlemann, J.: Excimerlaser ablation of fused silica. Appl. Surf. Sci. **54** (1992) p. 193–200.

[7] Lutz, N.; Geiger, M.: Processing of ceramics with excimer lasers. In: Bergmann, H. W.; Kupfer, R. (eds.): 3rd European Conference on Laser Treatment of Materials. Erlangen (Germany) 1990. Vol. 2. p. 849–857.

[8] Shinn, G. B.; Steigerwald, F.; Stiegler, H. et al.: Excimer laser photoablation of silicon. J. Vac. Sci. Technol. **B4** (1986) no. 6, p. 1273–1277.

[9] Buerhop, C.; Lutz, N.; Weißmann, R. et al.: Marking of silicate glasses with excimer laser radiation – Influence of glass and laser parameters. In: Mordike, B. L. (ed.): 4th European Conference on Laser Treatment of Materials, Göttingen (Germany) 1992. p. 603–608.

[10] Ihlemann, J.; Wolff, B.; Simon, P.: Nanosecond and femtosecond excimer-laser ablation of fused silica. Appl. Phys. **A54** (1992) p. 363–368.

[11] Geiger, M.; Lutz, N.; Goller, M.: Excimer laser radiation – A promising tool for microstructuring ceramics. Lasers Eng. (1993). (In prep.)

93R0246